JCB Article

Comparisons of CapG and gelsolin-null macrophages: demonstration of a unique role for CapG in receptor-mediated ruffling, phagocytosis, and vesicle rocketing

Walter Witke,[1] Wei Li,[2] David J. Kwiatkowski,[1] and Frederick S. Southwick[2]

[1]Hematology Division, Department of Medicine, Brigham and Women's Hospital, Boston, MA 02115
[2]Infectious Disease Division, Department of Medicine, University of Florida College of Medicine, Gainesville, FL 32610

Capping the barbed ends of actin filaments is a critical step for regulating actin-based motility in nonmuscle cells. The in vivo function of CapG, a calcium-sensitive barbed end capping protein and member of the gelsolin/villin family, has been assessed using a null *Capg* allele engineered into mice. Both CapG-null mice and CapG/gelsolin double-null mice appear normal and have no gross functional abnormalities. However, the loss of CapG in bone marrow macrophages profoundly inhibits macrophage colony stimulating factor–stimulated ruffling; reintroduction of CapG protein by microinjection fully restores this function. CapG-null macrophages also demonstrate ~50% impairment of immunoglobulin G, and complement-opsonized phagocytosis and lanthanum-induced vesicle rocketing. These motile functions are not impaired in gelsolin-null macrophages and no additive effects are observed in CapG/gelsolin double-null macrophages, establishing that CapG function is distinct from, and does not overlap with, gelsolin in macrophages. Our observations indicate that CapG is required for receptor-mediated ruffling, and that it is a major functional component of macrophage phagocytosis. These primary effects on macrophage motile function suggest that CapG may be a useful target for the regulation of macrophage-mediated inflammatory responses.

Introduction

The dynamic shifts in the concentration and length of actin filaments provide the force and structure for nonmuscle cell motility. A myriad of actin-binding proteins exists to temporally and spatially regulate actin filament assembly (Stossel, 1993). A key site for the regulation of actin filament assembly is the fast-growing or barbed (referring to the orientation of filaments when decorated with fragments of myosin) actin filament end. In living cells, the number of barbed ends available for the addition of actin monomers is likely to determine where new forces for directional cell movement are generated. Proteins capable of blocking exchange at the barbed end can prevent indiscriminate growth of actin filaments and control where new actin filaments are assembled. The gelsolin/villin family of actin regulatory proteins can serve this function (Kwiatkowski, 1999).

Gelsolin is the founding member of this family that now contains six members: gelsolin, villin, adseverin, CapG, advillin, and supervillin. These proteins all contain three to six homologous ancestral structural domains. Villin, advillin, and supervillin all have additional domains, and evidence suggests that they have specialized roles in the organization of actin filaments in the restricted cell types in which they are expressed. Gelsolin, adseverin, and CapG all have the common property of binding to the barbed end of actin filaments with high affinity. In addition, gelsolin and adseverin can both sever actin filaments in a diffusion-limited reaction, whereas CapG lacks this activity (Southwick and DiNubile, 1986).

Gelsolin is widely but not universally expressed in mammalian cells, whereas adseverin has a much more restricted expression pattern including certain lymphocytes and some adrenal, renal, and intestinal epithelial cell types (Maekawa and Sakai, 1990; Lueck et al., 1998). Gelsolin is highly expressed in platelets (Barkalow et al., 1996) and neutrophils, where it has been shown to be a critical element of a signal transduction cascade that results in rapid changes in the actin filament architecture.

CapG consists of only three ancestral structural domains, in contrast to the six present in gelsolin and adseverin (Yu et

Address correspondence to David Kwiatkowski, Division of Experimental Medicine, Brigham and Women's Hospital, Harvard Medical School, 221 Longwood Ave., Boston, MA 02115. Tel.: (617) 278-0384. Fax: (617) 734-2248. E-mail: dkwiatkowski@rics.bwh.harvard.edu

W. Witke's present address is EMBL, Mouse Biology Programme, 00016 Monterotondo-Scalo, Italy.

Key words: CapG; gelsolin; macrophages; ruffling; phagocytosis

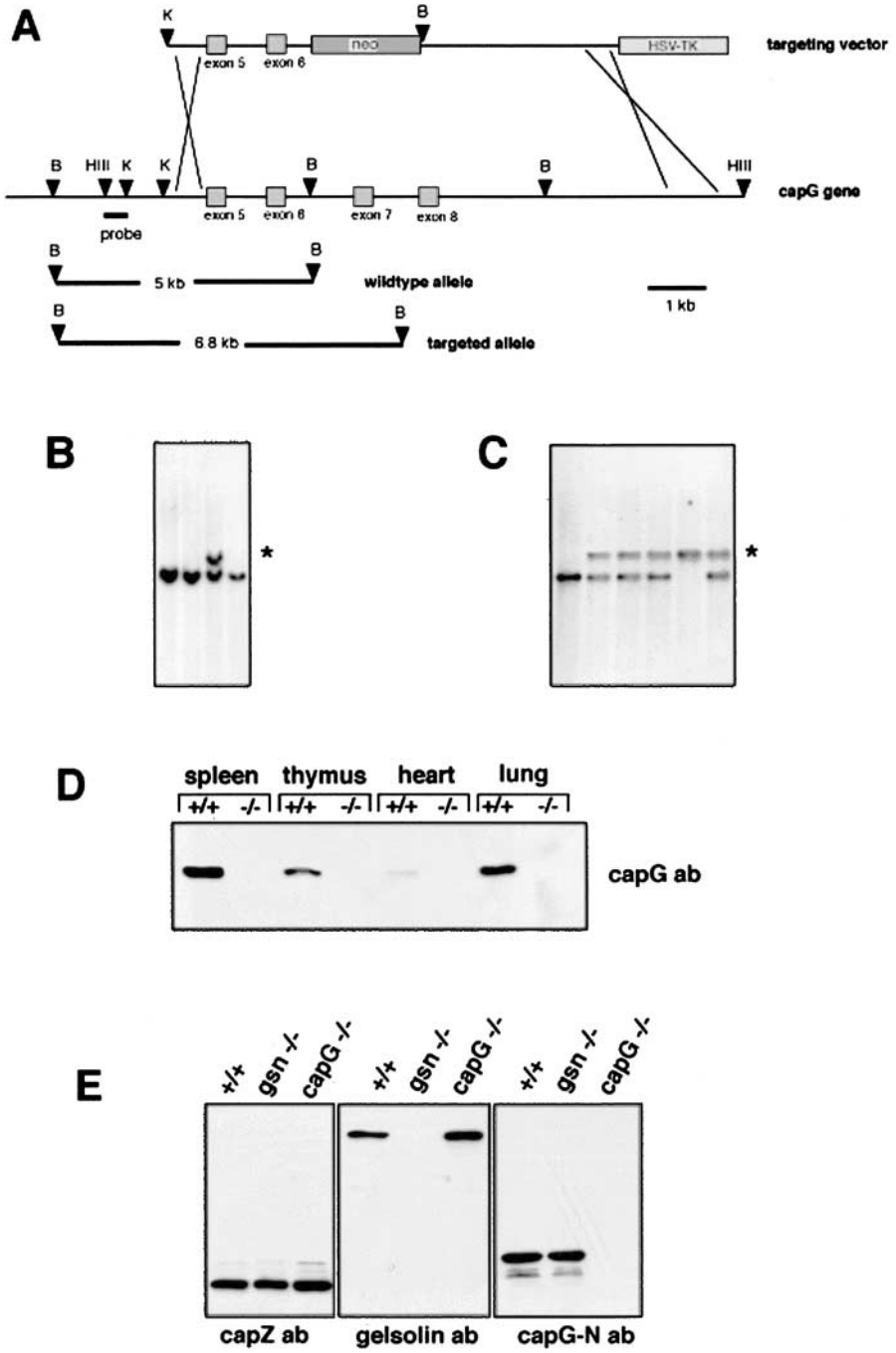

Figure 1. **Generation of *Capg*$^{-/-}$ mice.** (A) Diagram of the murine *Capg* gene and the gene-targeting construct. The probe used for Southern blot analysis and expected fragment sizes are indicated. (B and C) Southern blot analysis of BamHI-digested ES cell DNAs. The shifted 6.8-kb band (*) indicates that homologous recombination has occurred. (D) Southern blot analysis of DNAs derived from an intercross of mice each having a targeted *Capg* allele. One mouse is homozygous for the targeted allele. Immunoblot analysis of tissue extracts from wild-type and CapG-null mice using a rabbit IgG anti-CapG polyclonal antibody (ab). No CapG was detected in any tissue from the CapG-null mice. (E) Immunoblot analysis of macrophage extracts from wild-type, gelsolin-null, and CapG-null mice using antibodies against CapZ, gelsolin, and the NH_2 terminus of CapG. There is no significant difference in the concentrations of CapZ and gelsolin between wild-type and CapG-null cells, and no CapG signal of any size.

al., 1990; Prendergast and Ziff, 1991; Dabiri et al., 1992). CapG is found at levels comparable to gelsolin in many cell types. The concentrations of CapG differ from gelsolin in platelets where CapG is not detected, and in macrophages where CapG is more abundant than gelsolin, representing 1% of total cytoplasmic protein (Dabiri et al., 1992).

Another characteristic shared by gelsolin and CapG is regulation of their actin-binding activity by micromolar Ca^{2+}. Both proteins are activated by micromolar Ca^{2+}, and in the case of CapG this activation is reversible by reducing Ca^{2+}. That is, when Ca^{2+} is lowered to the submicromolar range, CapG rapidly dissociates from the barbed end. In contrast, gelsolin does not release actin in submicromolar Ca^{2+}, but rather phosphoinositide binding is required for release (Janmey et al., 1985). The reversibility of CapG binding raises the possibility that this capping protein may regulate actin filament length in response to fluctuations in intracellular calcium. Ruffling, an actin-based movement that coincides with Ca^{2+} oscillations, is a potential candidate for CapG regulation.

Determining the relative contribution of each actin regulatory protein to actin dynamics in the living cell is a clear challenge. In the cell, actin filament barbed ends may be regulated by any of the members of the gelsolin family as well as the ubiquitously expressed CapZ (Cooper and Schafer, 2000). We previously pursued this challenge by generating mice null for expression of gelsolin. Gelsolin-null mice demonstrate normal reproductive function and appear grossly normal. However, detailed analysis of multiple organs and cell types have revealed a wide range of defects in these mice, from prolonged bleeding times due to defective platelet

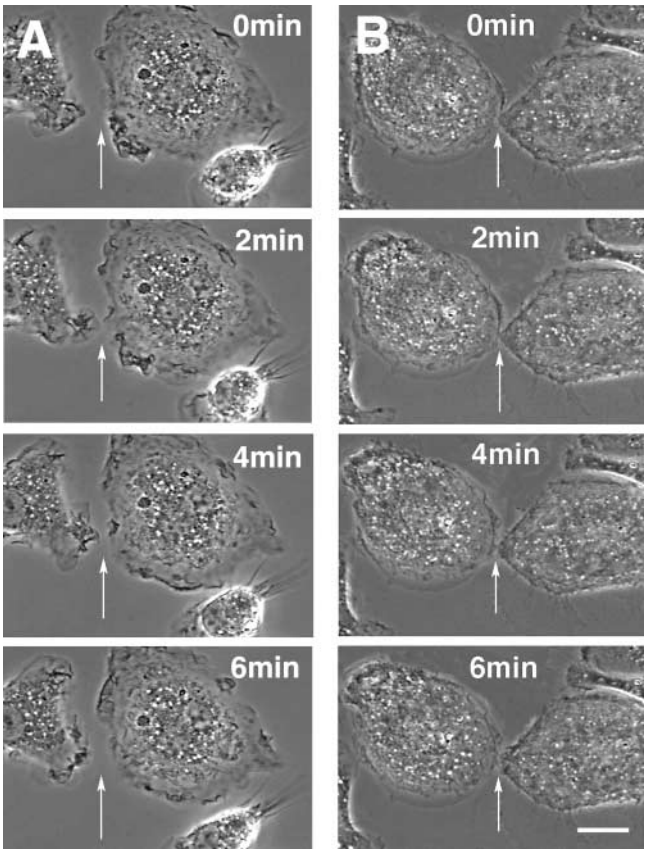

Figure 2. **Spontaneous ruffling response of (A) wild-type and (B) CapG-null mouse bone marrow macrophages demonstrated by time-lapse phase microscopy.** Images were obtained at 10-s intervals. Note the marked changes in the peripheral membrane of wild-type cells (see arrow) compared with CapG-null macrophages.

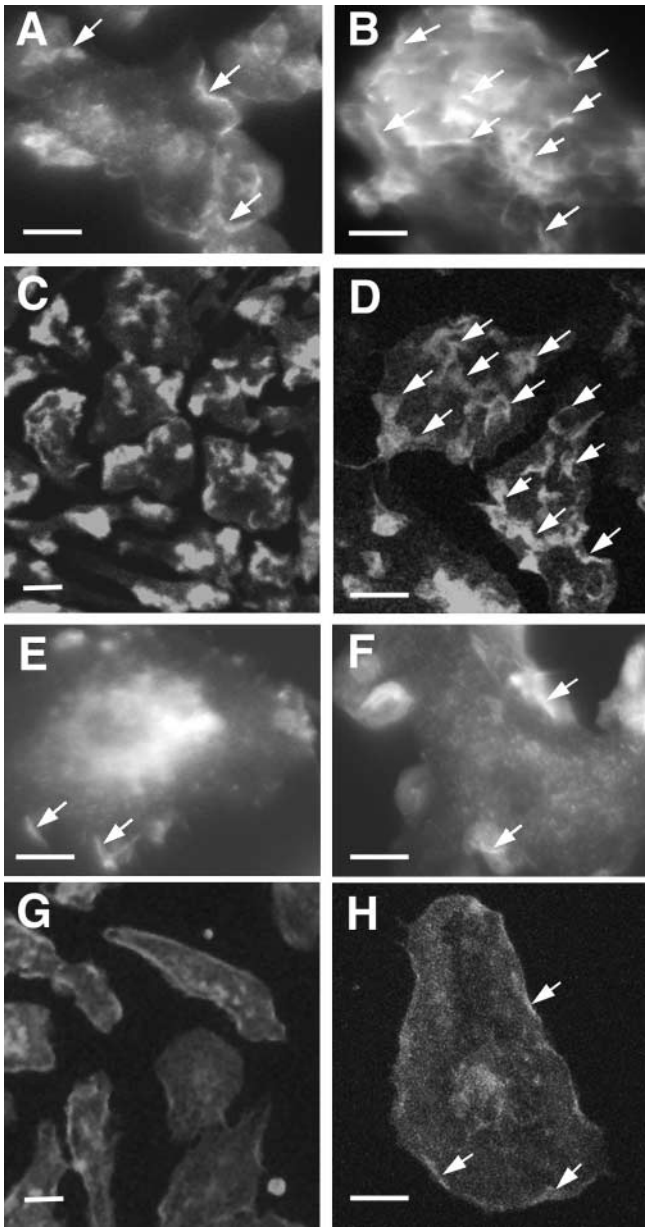

Figure 3. **Effects of MCSF on the ruffling response of wild-type and *Capg*$^{-/-}$ macrophages.** Phalloidin staining of wild-type (A–D) and CapG-null (E–H) macrophages before and after exposure to MCSF. Cells were fixed and stained with rhodamine-phalloidin either before or 5 min after exposure to MCSF. Images C, D, G, and H are confocal images; C and G are representative lower power views. Note the increase in serpentine staining indicative of ruffling (arrows) in cells exposed to MCSF compared with unstimulated cells in wild-type, but not in *Capg*$^{-/-}$ cells. Bars, 10 mm.

shape changes, to impaired breast ductal morphogenesis (Kwiatkowski, 1999; Crowley et al., 2000).

To assess the critical functions of CapG in actin dynamics and cell physiology, we have generated a null allele of *Capg* in the mouse. As observed with the gelsolin-null animals, CapG-null mice demonstrate normal reproductive function and appear grossly normal. However, analysis of CapG-null macrophages points to the critical role of CapG in actin-based motility in vivo, and investigations of gelsolin/CapG double-null cells reveal that gelsolin and CapG serve distinct, nonoverlapping functions in macrophages.

Results

Targeted disruption of the *CAPG* gene

An 11-kb HindIII fragment of the murine *CAPG* gene was identified that contained exons 5–8. To generate an inactivating mutation, exons 7 and 8 were deleted and replaced by a neomycin resistance cassette (*neo*^{r}). The herpes simplex virus thymidine kinase cassette was then positioned on the 3′ side of the construct for negative selection (Fig. 1 A). After electroporation into J1 embryonic stem (ES)* cells, 135 clones were selected by resistance to G418 and 1-2′-deoxy-2′-fluoro-β-D-arabinofuranosyl-5-iodouracil. Southern blot analysis using a flanking probe showed that homologous recombination with the native CapG locus had occurred in a single ES cell clone (Fig. 1 B). This ES cell clone was injected into BalbC blastocysts, chimeras were obtained, and transmission of the targeted allele in successive breedings was confirmed by Southern blot analysis (Fig. 1 C). Offspring generated by intercrosses of mice bearing the targeted *Capg* allele demonstrated Mendelian segregation, indicating

*Abbreviations used in this paper: $[Ca^{2+}]_I$, intracellular $[Ca^{2+}]_I$; ES, embryonic stem; MCSF, macrophage colony stimulating factor; PAF, platelet-activating factor; PIP_2, phosphatidylinositol 3,4 or 4,5-bisphosphate.

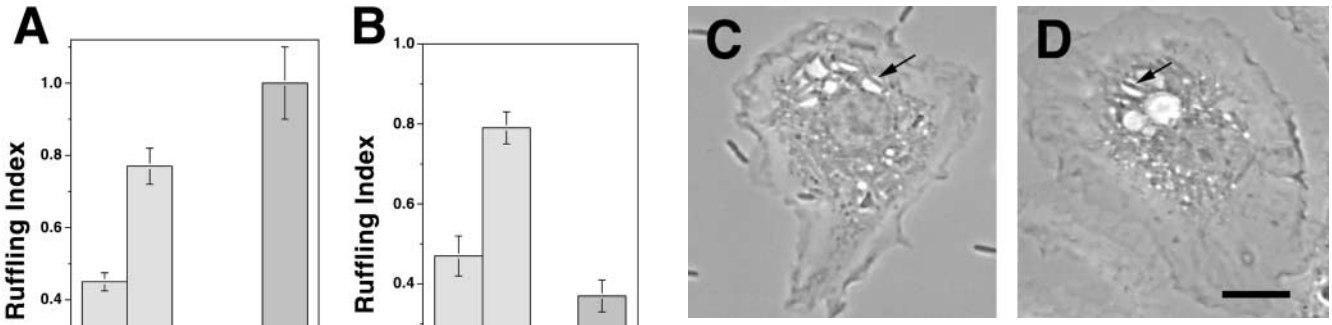

Figure 4. **Quantitation of the ruffling responses of wild-type and *Capg*$^{-/-}$ macrophages.** (A) Bar graphs comparing the ruffling indexes of wild-type and *Capg*$^{-/-}$ macrophages before and after exposure to MCSF. The ruffling index was determined based on analysis of phalloidin staining by a blinded observer (Materials and methods). In the first four bars, brackets represent the SEM for 80–100 determinations/condition. Wild-type cells have a higher spontaneous ruffling index and nearly double their ruffling activity in response to MCSF, whereas *Capg*$^{-/-}$ macrophages have a lower spontaneous ruffling activity and fail to respond to MCSF. The far right bar quantifies the ruffling activity of *Capg*$^{-/-}$ cells stimulated with MCSF after introduction of recombinant CapG by microinjection. Bracket represents the SEM of $n = 34$ cells. CSF, MCSF. (B) Bar graphs comparing the ruffling responses of wild-type and *Capg*$^{-/-}$ macrophages after exposure to *Salmonella* (Salm.). Unlike MCSF which failed to stimulate ruffling in *Capg*$^{-/-}$ macrophages, exposure to *Salmonella* resulted in a significant increase in ruffling activity ($P < 0.0001$). Brackets represent the SEM of $n = 80$–100 measurements. Cells were scored as described in A. (C and D) Phase micrographs of wild-type (C) and *Capg*$^{-/-}$ (D) macrophages after 30-min exposure to *Salmonella*. Note the giant phagolysosomes in both the wild-type and *Capg*$^{-/-}$ cells induced by exposure to the bacteria. Arrows point to individual bacteria contained in giant phagolysosomes. Bar, 10 mm.

that mice homozygous for the targeted allele were viable (see below).

Analysis of CapG expression in the targeted mice

In contrast to wild-type tissues, *Capg* mRNA was undetectable by Northern blot analysis of spleen, lung, thymus, kidney, and heart RNA from mice homozygous for the targeted allele (unpublished data). Moreover, no CapG was detected by immunoblot analysis of spleen, thymus, lung, and heart extracts derived from mice homozygous for the targeted *Capg* allele, in contrast to control samples from wild-type mice (Fig. 1 D). To exclude the possibility that *CapG*-null cells might express an NH_2-terminal–truncated version of CapG, we performed immunoblot analyses of bone marrow–derived macrophages using a polyclonal rabbit antibody directed against the NH_2-terminal half of CapG. No reactive bands of lower molecular mass were seen (Fig 1 E). As a control, the expression of CapZ and gelsolin were also analyzed in these macrophage extracts (Fig. 1 E). High-level expression was detected as expected, but there was no increase in expression of these functionally related proteins in extracts from macrophages that were homozygous for the targeted *Capg* allele. Based on these data, we designate the targeted allele as a null allele for *Capg* (*Capg*$^{-}$).

Viability, fertility, and general pathology

Interbreeding of *Capg*$^{+/-}$ animals yielded the expected number of *Capg*$^{-/-}$ offspring, according to Mendelian segregation ratios (30 *Capg*$^{+/+}$, 79 *Capg*$^{+/-}$, 29 *Capg*$^{-/-}$, $P > 0.1$). The oldest *Capg*$^{-/-}$ mice have reached the age of 2 yr with no apparent morbidity, compared with wild-type littermates. Histologic analyses of the bone marrow, brain, gastrointestinal tract, liver, heart, lungs, kidneys, spleen, lymph nodes, and thymus from 3-mo-old *CapG*$^{-/-}$ mice revealed no gross or microscopic abnormalities. Analysis of peripheral blood counts demonstrated normal leukocyte, red blood cell, and platelet counts as follows: peripheral white blood cells, 1.9–2.8 $\times$ $10^3/\mu$l for wild-type (+/+) vs. 1.4–2.45 $\times$ $10^3/\mu$l for *Capg*-null (−/−) mice; red blood cells, 8.1–8.2 $\times$ $10^6/\mu$l (+/+) vs. 7.8–8.0 $\times$ $10^6/\mu$l (−/−); platelets, 705–850 $\times$ $10^3/\mu$l (+/+) vs. 703–957 $\times$ $10^3/\mu$l (−/−). The percentage of peripheral neutrophils, lymphocytes, and mononuclear cells was also similar in wild-type and CapG-null mice.

Neutrophils and fibroblasts

In *Gsn*$^{-/-}$ mice, neutrophil migration to the peritoneum was delayed after the instillation of thioglycolate as an inflammatory stimulus (Witke et al., 1995). In *Capg*$^{-/-}$ mice there was a slight reduction in neutrophil migration, but this difference did not achieve statistical significance. Due to a defect in rac signaling, gelsolin-null dermal fibroblasts have prominent stress fibers that persist despite serum starvation (Azuma et al., 1998). A similar study of *Capg*$^{-/-}$ fibroblasts demonstrated normal stress fiber formation, as assessed by rhodamine-conjugated phalloidin staining during both normal growth and serum starvation (unpublished data).

Bone marrow macrophages

Because macrophages contain the highest concentrations of CapG of any cell, we examined the structure and motility of *Capg*$^{-/-}$ macrophages in detail.

Ruffling. Dynamic changes in intracellular [Ca^{2+}] are associated with macrophage ruffling, and CapG's affinity for actin is regulated in a similar [Ca^{2+}] range; therefore, we

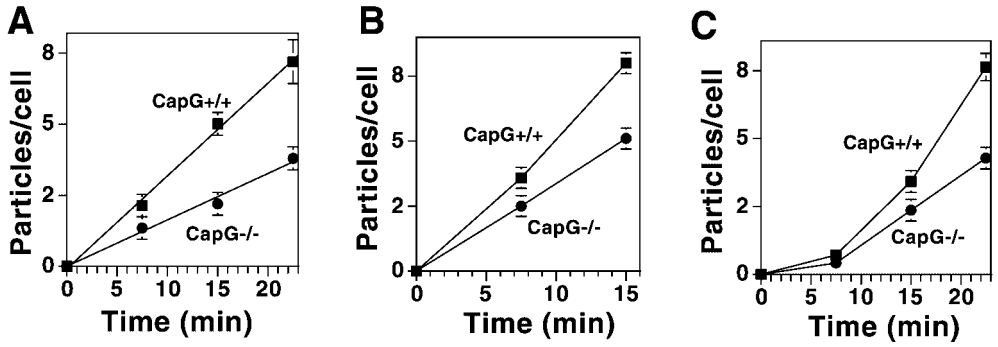

Figure 5. **Phagocytic rates of wild-type and *Capg*$^{-/-}$ macrophages.** (A) Line graph quantitating the number of IgG-opsonized zymosan particles ingested over time. Macrophages were exposed to the opsonized zymosan particles and at the times depicted were cooled to 4°C. Cells were overlaid with Trypan blue to quench extracellular particles and the number of particles inside each cell were counted. Brackets represent the SEM of 90–100 cells counted per time point. The slope of the *Capg*$^{-/-}$ cells was half that of wild-type cells. (B) Line graph quantitating the number of complement-opsonized zymosan particles ingested over time. Brackets represent the SEM of 100 cells per time point. The slope was reduced by approximately 35% in the *Capg*$^{-/-}$ cells. Wild-type cells failed to ingest additional particles at 22.5 min (mean particles/cell 8.8 ± 0.3; $n = 100$) Therefore, meaningful comparisons between wild-type and *Capg*$^{-/-}$ cells could not be made at this time point. (C) Line graph quantitating the number of unopsonized zymosan particles ingested over time. No significant ingestion was observed at 7.5 min. Brackets represent the SEM of 100 cells/time point.

used time-lapse microscopy to examine macrophage ruffling. A qualitative decrease in spontaneous ruffling was observed in *Capg*$^{-/-}$ macrophages (Fig. 2). To provide a more quantitative score of ruffling activity we used rhodamine-phalloidin staining and fluorescence microscopy. It has previously been shown that localized increases in actin filaments occur at the site of ruffling that appear as a serpentine pattern of rhodamine-phalloidin staining (Cox et al., 1997; Heidemann et al., 1999). A reduction in the spontaneous ruffling activity of null compared with wild-type macrophages was apparent (compare Fig. 3, A with E), and this difference was markedly accentuated by a 5-min exposure to macrophage colony stimulating factor (MCSF) (compare Fig. 3, B–D with F–H). These differences were quantitated to calculate a ruffling index for each set of cells by a blinded observer (see Materials and methods). *Capg*$^{-/-}$ macrophages had a ruffling index that was <1/2 the ruffling index of wild-type cells ($P < 0.001$) (Fig. 4 A). After exposure to MCSF, the ruffling index of *Capg*$^{-/-}$ macrophages did not change, whereas that of wild-type cells increased by nearly 70% (Fig. 4 A). The lack of response to MCSF was a consistent finding, seen in four of four separate experiments.

To confirm that the decrease in spontaneous and MCSF-stimulated ruffling of *Capg*$^{-/-}$ macrophages was due to a lack of CapG and not some other genomic event or compensatory expression effect, we added CapG back by microinjection. CapG was microinjected (30 mg/ml needle concentration, estimated intracellular concentration 3 mg/ml or 7.9 μM), and 30 min after microinjection the *Capg*$^{-/-}$ cells were stimulated with MCSF. Introduction of CapG resulted in a marked increase in ruffling activity in response to MCSF, mean ruffling activity exceeding that of wild-type cells (Fig. 4 A). This greater than normal ruffling activity may reflect the higher than normal concentrations of CapG present in some cells after microinjection.

Second, we examined the ruffling activity of *CapG*$^{-/-}$ macrophages in response to incubation with *Salmonella typhimurium*. This bacterium injects proteins into the cytoplasm of cells, bypassing membrane receptors and inducing the formation of giant ruffles (Rudolph et al., 1999; Zhou et al., 1999). Ruffling is accompanied by ingestion of bacteria and the formation of giant phagolysosomes (Jones et al., 1993; Alpuche-Aranda et al., 1994; Garcia-del Portillo and Finlay, 1994). *Capg*$^{-/-}$ macrophages responded to *Salmonella* exposure by significantly increasing their ruffling activity ($P < 0.0001$) (Fig. 4 B). Although the basal and maximal ruffling activities were lower than wild-type macrophages, *Capg*$^{-/-}$ cells did increase their ruffling index by three times, the same relative increase as wild-type cells. Both groups of cells demonstrated giant phagolysosomes that contained bacteria (Fig. 4, C and D).

Phagocytosis. The ability of bone marrow macrophages to ingest complement- and IgG-opsonized, as well as unopsonized fluorescein-labeled zymosan particles was also examined. The rates of IgG-mediated phagocytosis were decreased to ~1/2 that of wild-type cells (Fig. 5 A, $P < 0.0001$ at 15 and 22.5 min). Similarly, complement-mediated phagocytosis was decreased, although to a lesser degree (Fig. 5 B, $P < 0.0001$ at 7.5 and 15 min). *Capg*$^{-/-}$ macrophages also demonstrated significantly slower rates of ingestion of unopsonized particles compared with wild-type macrophages ($P = 0.005$ at 15 min and $P < 0.0001$ at 22.5 min) (Fig. 5 C). The reduction in phagocytic rate of IgG-coated particles could not be accounted for by a difference in particle adherence. The mean number of IgG-opsonized particles attached to CapG-null macrophages (0.7 ± 0.1 particles/cell SEM, $n = 100$ cells) after incubation at 37°C for 22 min was not significantly different than wild-type macrophages (0.9 ± 0.1 particles/cell; $n = 100$, $P = 0.14$).

Vesicle rocketing. When wild-type macrophages were exposed to lanthanum hydrogen chloride for 10 min followed by zinc, these cells formed multiple vesicles within their cytoplasm (see Materials and methods). After 20–30 min, ~2% of the vesicles began moving within the cytoplasm at velocities ranging from 0.05 to 0.12 μm/s. Movement was associated with the formation of actin filament tails (Zeile et al., 2000). Similar treatment of *Capg*$^{-/-}$ macrophages led to the

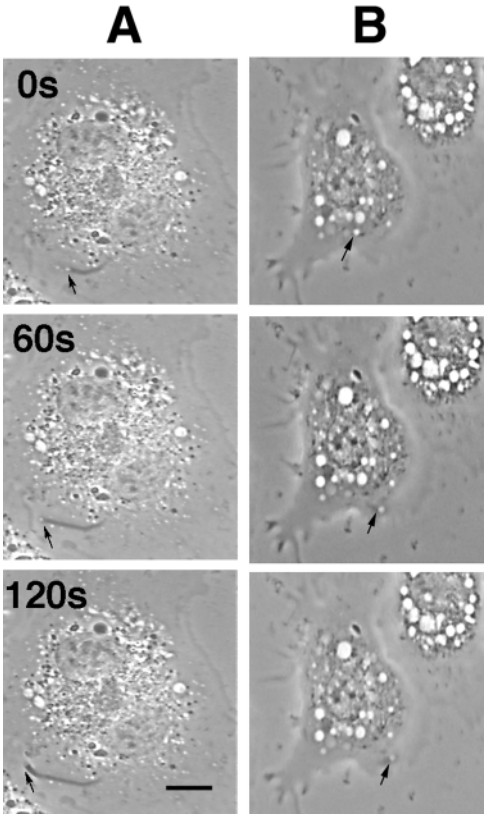

Figure 6. **Time-lapse phase micrographs of endosomal rocketing in wild-type and *Capg*$^{-/-}$ macrophages.** Cells were treated with lanthanum and zinc chloride as described in the Materials and methods. This treatment induces the formation of vesicles that move through the cytoplasm by an actin-based motor. (A) The left-hand column shows a vesicle rocketing through a wild-type macrophage (arrow). (B) The right-hand column shows a vesicle migrating through a *Capg*$^{-/-}$ macrophage (arrow). Time is depicted in the upper left-hand corner. Note the long phase-dense actin tail in the wild-type cell (A) and the very short actin tail in the Capg$^{-/-}$ cell (B). Phase-dense tails were rarely seen behind rocketing vesicles in *Capg*$^{-/-}$, but were commonly seen in wild-type cells. The average velocity of rocketing vesicles in *Capg*$^{-/-}$ macrophages was <1/2 that of wild-type cells. Bar, 10 mm.

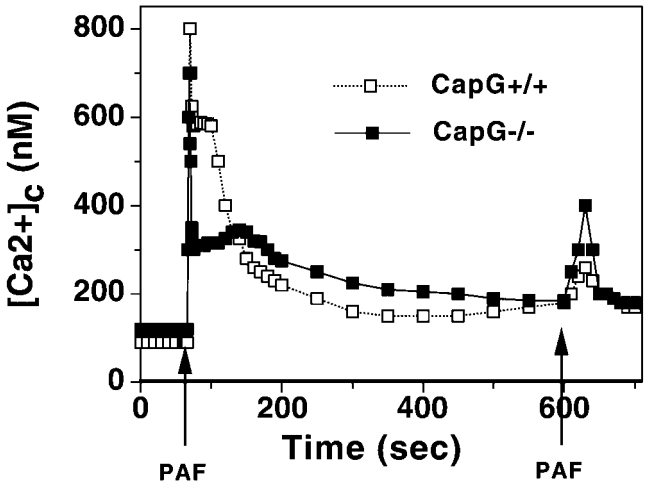

Figure 7. **Cytosolic [Ca^{2+}] changes in wild-type and *Capg*$^{-/-}$ macrophages after stimulation with PAF.** Adherent macrophages were loaded with Fura-2 as described in the Materials and methods, and fluorescence was monitored over time. Intracellular Ca^{2+} was calibrated as described in the Materials and methods. Arrows depict the time point when a final concentration of 20 ng/ml of PAF was added to the buffer. This experiment is representative of 7 determinations in wild-type and 10 determinations in *Capg*$^{-/-}$ macrophages. The peak $[Ca^{2+}]_I$ was 800 nM in wild-type and 750 nM in *Capg*$^{-/-}$ cells.

formation of fewer vesicles compared with wild-type macrophages, although this difference did not achieve statistical significance (mean of 46 ± 7.4 vesicles/*Capg*$^{-/-}$ cell vs. 77 ± 23/wild-type cell; n = 12–17 cells, P = 0.184). However, phase-dense rocket tails were shorter or absent in *Capg*$^{-/-}$ cells (Fig. 6) and the velocities of motile vesicles were less than half that of wild-type cells (mean of 0.08 ± 0.002 μm/s, n = 93 vs. *Capg*$^{-/-}$ cells 0.03 ± 0.002 μm/s; n = 66, $P < 0.0001$).

Cytosolic-free Ca^{2+}. Using Fura-2 as an indicator, we have examined the ability of wild-type and *Capg*$^{-/-}$ macrophages to respond to the agonist platelet-activating factor (PAF). This inflammatory mediator binds to a specific receptor whose signal transduction is mediated through G proteins and phosphoinositides (Mazer et al., 1992). As shown in Fig. 7, *Capg*$^{-/-}$ cells responded with a rapid rise in intracellular [Ca^{2+}] ($[Ca^{2+}]_I$) that was comparable to wild-type macrophages. Wild-type cells demonstrated a more persistent elevation in $[Ca^{2+}]_I$ than null cells. However, over time, resting values reached comparable levels and after a second exposure to PAF, null cells responded with a second rise in $[Ca^{2+}]_I$ that was somewhat greater than wild-type cells.

Analysis of double knockout macrophages lacking both CapG and gelsolin

Given the close structural and functional similarities between gelsolin and CapG, we hypothesized that the in vivo functions of the two proteins might overlap, and that double-null *Capg*$^{-/-}$*Gsn*$^{-/-}$ mice could have a more severe phenotype than either *Gsn*$^{-/-}$ or *Capg*$^{-/-}$ mice. *Capg*$^{-/-}$*Gsn*$^{-/-}$ mice were obtained by breeding. Longitudinal observation and pathological exam in these double knockout mice demonstrated no obvious phenotype, similar to the single-null mice. Using these same assays, we then examined the motility of macrophages derived from mice with each of these three genetic constitutions.

Ruffling. In contrast to *Capg*$^{-/-}$ macrophages, *Gsn*$^{-/-}$ macrophages had somewhat increased spontaneous and CSF-induced ruffling activity compared with wild-type cells, although this difference did not achieve statistical significance. Double-null *Capg*$^{-/-}$*Gsn*$^{-/-}$ macrophages displayed spontaneous and MCSF-induced ruffling activity that was nearly identical to that of *Capg*$^{-/-}$ macrophages (Fig. 8 A).

Phagocytosis. *Gsn*$^{-/-}$ macrophages phagocytosed IgG-coated zymosan particles at a rate virtually identical to wild-type cells (Fig. 8 B). Double-null *Capg*$^{-/-}$*Gsn*$^{-/-}$ macrophages demonstrated rates of phagocytosis that were indistinguishable from *Capg*$^{-/-}$ macrophages. Studies performed using zymosan particles opsonized with complement yielded similar results (unpublished data).

Vesicle rocketing. As observed for phagocytosis and ruffling, gelsolin deletion failed to impair vesicle rocketing.

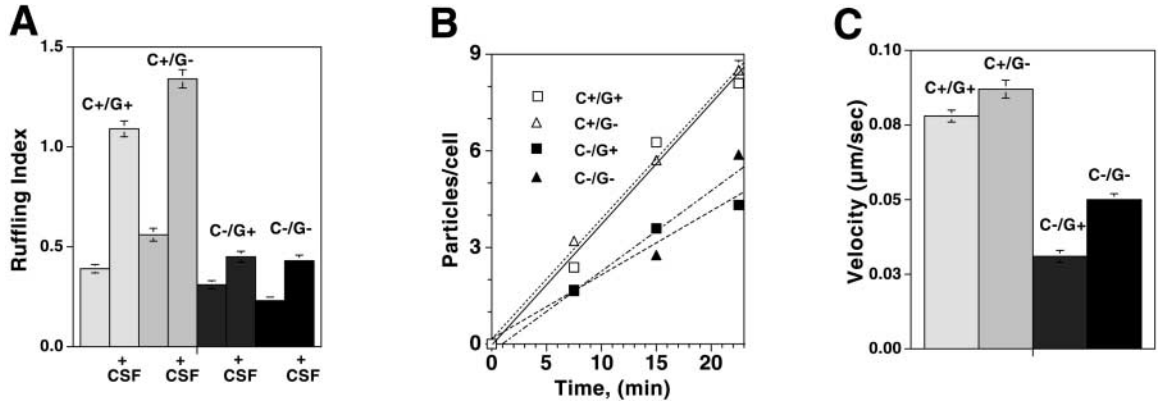

Figure 8. **Comparisons of wild-type, *Gsn*$^{-/-}$, *Capg*$^{-/-}$, and *Gsn*$^{-/-}$/*Capg*$^{-/-}$ bone marrow macrophages.** Removal of gelsolin failed to significantly impair any of the motile functions tested. (A) Bar graphs comparing the ruffling indexes of all four types of macrophages before and after exposure to MCSF. Brackets represent the SEM of $n = 90–100$ cells for each group. (B) Line graphs comparing the phagocytic rate for IgG-opsonized zymosan ingestion in the four cell types. Brackets represent the SEM of $n = 90–100$. (C) Bar graphs comparing the vesicle rocket velocities in the four cell types. Brackets represent the SEM of $n = 90–100$. C, Capg; G, Gsn.

Gsn$^{-/-}$ macrophages displayed a mean vesicle velocity that was somewhat higher than wild-type cells, and this difference was statistically significant ($P = 0.036$) (Fig. 8 C). Similarly, the vesicles of double-null *Capg*$^{-/-}$*Gsn*$^{-/-}$ macrophages had a significantly higher velocity than vesicles in *Capg*$^{-/-}$ macrophages ($P < 0.0001$) (Fig. 8 C).

Discussion

Capping of the barbed ends of actin filaments is a key control step in the regulation of actin polymerization. Given the likely importance of this regulatory step, it is not surprising that nonmuscle cells contain many barbed end capping proteins. The ability of multiple proteins to serve this function is likely to explain why loss of CapG and/or gelsolin does not have lethal effects in mice, at least in mixed genetic backgrounds. In particular, the most evolutionarily conserved barbed end capping protein, the original "capping protein," CapZ, may serve to regulate the motile functions required for embryonic development. CapZ is expressed in virtually all mammalian cell types, and similar to CapG and gelsolin, its affinity for the barbed end is regulated by phosphoinositides of the D4 type, particularly phosphoinositide 3,4-bisphosphate (PIP_2) (Schafer et al.,1996). However, in contrast to both gelsolin and CapG, CapZ is not regulated by [Ca^{2+}]. Loss of CapZ has near lethal effects in yeast (Amatruda et al., 1990), suggesting that it is also required for viability in mammals. Our analysis of CapG and gelsolin/CapG double-null mice indicate that these two proteins are not absolutely required for viability, and that their loss yields a grossly normal phenotype with apparently normal reproductive capabilities.

Given the multiplicity of barbed end capping proteins, cell biologists have been unable to determine how these individual proteins contribute to cell motility. Do they simply serve redundant functions, or do specific capping proteins regulate specific motile functions? Previous studies of gelsolin knockout cells suggest that this protein regulates the morphology of fibroblast stress fibers, facilitates the wound healing response of fibroblasts, and enhances chemotaxis of neutrophils. Gelsolin is most abundant in platelets, and knockout studies suggest that gelsolin's most prominent role involves platelet function. Gelsolin-null platelets demonstrate defective actin remodeling resulting in impaired spreading (Witke et al., 1995). Many other defects have also been described in gelsolin-null mice and their cells (Kwiatkowski, 1999).

CapG is also conserved throughout all vertebrate species. It is expressed at moderately high levels in most cell types (except platelets), and is an abundant protein in macrophages (Dabiri et al., 1992). Therefore, it is not surprising that CapG-null macrophages demonstrate marked defects in actin-based motile function. Macrophages are one of the most dynamic cells in the body. The dorsal surface of adherent macrophages rapidly changes shape, quickly forming outward protrusions of the peripheral membrane often termed ruffles. The rate of ruffling tends to closely correlate with the transient rise and fall of intracellular calcium, suggesting that this process is Ca^{2+} sensitive. Ruffling is known to result from localized actin filament assembly (Heidemann et al., 1999), and because CapG is the only known reversibly calcium-sensitive capping protein, we hypothesized that this protein might play a key role in regulating the ruffling response (Southwick and DiNubile, 1986). Our investigations of *Capg*$^{-/-}$ macrophages now support this hypothesis. Compared with wild-type macrophages, CapG-null macrophages have decreased spontaneous ruffling and show no ruffling response to MCSF. CapG-associated ruffling is likely to be linked to MCSF receptor activation because stimulation of ruffling by *Salmonella*, a stimulus that bypasses this surface receptor, causes comparable relative increases in the ruffling activity of wild-type and CapG-null macrophages. The decrease in *Capg*$^{-/-}$ macrophage ruffling response to MCSF could be caused by a decrease in phosphoinositide turnover and a reduction in the receptor-mediated rise in intracellular Ca^{2+}. CapG binds PIP_2 with high affinity, and overexpression of CapG has been associated with increased receptor-mediated phosphoinositide turnover and Ca^{2+} signaling (Sun et al., 1995). Loss of CapG could have the opposite effect. To explore this possibility we measured Ca^{2+} signaling

in response to the inflammatory mediator PAF. Binding to the PAF receptor has previously been shown to stimulate phosphoinositide turnover and a rise in intracellular [Ca^{2+}] (Mazer et al., 1992). *Capg*$^{-/-}$ macrophages responded with a peak rise in [Ca^{2+}]$_I$ comparable to wild-type cells, excluding a significant defect in calcium signaling.

Gelsolin could also play a role in the ruffling activity of macrophages through its actin filament severing and barbed end capping activities. Analysis of gelsolin-null macrophages as well as macrophages lacking both CapG and gelsolin indicates that gelsolin plays no significant role in ruffling. In fact, gelsolin-negative cells tended to have a more prominent ruffling response in the presence of CapG. It is puzzling that loss of gelsolin fails to impair actin-based motility in macrophages. This is particularly striking in view of the high level of expression of gelsolin in these cells. The results imply that gelsolin's severing activity is not required for the motility observed. The increase in ruffling in the absence of gelsolin may reflect gelsolin's inhibition of signaling through phosphoinositides in wild-type cells, given gelsolin's high affinity for these compounds, or a loss of gelsolin's capping activity, which might inhibit ruffling activity.

In addition to ruffling, macrophages are capable of quickly forming pseudopods to ingest and destroy foreign particles. This function would also be expected to require barbed end actin filament assembly and cytochalasins, agents that block assembly at this end and that are known to block phagocytosis (Hartwig and Stossel, 1976). Our experiments indicate that CapG plays a significant role in macrophage phagocytosis. Unlike MCSF-stimulated ruffling which is totally abrogated by the loss of CapG, phagocytosis is decreased by half, indicating that other actin regulatory proteins contribute to this process. Our investigations of double knockout cells, as well as gelsolin-null cells, reveal that gelsolin does not significantly contribute to phagocytosis of opsonized zymosan particles in macrophages. In murine neutrophils, gelsolin has been shown to play a significant role in the phagocytosis of IgG-opsonized yeast particles, but its loss has no significant effect on complement-mediated ingestion (Serrander et al., 2000). These observations suggest that actin regulatory proteins may serve different functions in even closely related cell types.

Finally, CapG appears to play a role in vesicle rocketing in macrophages. When macrophages are treated with lanthanum followed by zinc, a small percentage of the resulting vesicles begin to move through the cytoplasm, being propelled by actin filament rocket tails (Zeile et al., 2000). Although the exact origin of these activated membranes remains to be defined, their movement requires the assembly of actin filaments at their barbed ends, and loss of CapG clearly results in a marked reduction in the speed of endosomal migration, indicating that CapG facilitates this process. Additional experiments are planned to explore this mechanism in more detail. As observed with ruffling and phagocytosis, gelsolin deletion did not slow the velocity of rocketing.

How could CapG serve to enhance these actin-based motile functions? In vitro studies demonstrate that the ability of CapG to cap the barbed ends of actin filaments is blocked by lowering Ca^{2+} to the nanomolar range (Young et al., 1994), and by increasing concentrations of PIP_2 micelles to the submicromolar range (Yu et al., 1990). Receptor-induced cyclic changes in [Ca^{2+}] and/or local [PIP_2] would be expected to alternatively activate and inactivate CapG. A reduction in intracellular [Ca^{2+}] below the micromolar range or increases in local [PIP_2] could inactivate CapG and uncap barbed ends, allowing actin filament growth and membrane protrusion. Increasing intracellular [Ca^{2+}] to the micromolar range or reduction in local [PIP_2] would allow CapG to cap the barbed filament ends. This condition would be expected to cause net filament depolymerization and peripheral membrane retraction. Loss of CapG would block the ability of these second messengers to regulate actin filament capping, and may explain the loss of receptor-mediated membrane ruffling in CapG-null macrophages. Regulation of barbed end filament growth could also serve to discretely regulate actin filament growth in regions of new pseudopod formation and during vesicle rocketing. As proposed in *Listeria* actin-based motility (Sechi et al., 1997), the capping of filaments whose barbed ends grow laterally outside of the polymerization zone would serve to prevent misdirected actin filament growth, and thereby allow the more efficient production of directional force for pseudopod formation and vesicle movement.

Investigators need to keep in mind that whenever a single gene is deleted, other adaptations may occur, including upregulation of G proteins and changes in the concentrations of other related proteins. Although we have excluded significant changes in the concentrations of known mammalian capping proteins, we cannot exclude the possibility that secondary adaptive changes may at least partially account for the resulting phenotype. However, the finding that microinjection of CapG into null macrophages rapidly and fully restores actin-based ruffling provides strong evidence for CapG's central role in this motile process. One must also keep in mind that CapG may have other undiscovered properties in addition to barbed end capping of actin filaments and phosphoinositide binding that could contribute to the restoration of ruffling in macrophages.

In summary, our analysis of mice and their macrophages engineered to be null for CapG expression demonstrates that CapG serves important functions in actin-based macrophage motility that are distinct from those of gelsolin. CapG is required for receptor-mediated ruffling, facilitates IgG complement and unopsonized zymosan phagocytosis, and accelerates the motility of vesicle rockets. These processes are likely to play critical roles in host defense and immunity, and CapG may prove to be a useful target for the regulation of inflammation.

Materials and methods

Generation of *CAPG*$^{-}$ ES cells and mice

The murine *CAPG* genomic fragment was isolated from a murine genomic EMBL3 lambda library constructed from 129Sv genomic DNA (Witke et al., 1995) using the human CapG cDNA as a probe. Three pseudogenes were identified in the course of characterizing the authentic CapG locus. An 11-kb KpnI-HindIII CapG genomic fragment containing exons 5–8 was cloned, and an internal BamHI fragment (containing exons 7 and 8) was replaced with a neomycin resistance construct. This fragment was then inserted into a vector containing the herpes simplex virus thymidine kinase gene to provide negative selection. The vector was linearized with SalI and transfected by electrocorporation into 10^7 J1 ES cells (Li et al., 1992),

which were maintained on a feeder layer of *neo*^{r} embryonic fibroblasts in the presence of 500 U/ml of leukemia inhibitory factor. 135 clones were selected with G418 (200 μg/ml) and 1-2′-deoxy-2′-fluoro-β-D-arabinofuranosyl-5-iodouracil (2 μM). After minimal passage, the DNA prepared from the clones was analyzed by Southern blot using an adjacent 0.3-kb Kpn fragment (Fig. 1). One clone demonstrated evidence for homologous recombination, and was injected into BalbC blastocysts which were then transferred to pseudopregnant foster mothers, and chimeric offspring obtained. F1 mice obtained from chimeric matings were genotyped by Southern blot analysis of DNA isolated from tail biopsies, and were crossed to obtain homozygous CapG mutant mice.

DNA preparations and Southern blot analysis were performed by standard methods, including labeling of DNA probes using [^{32}P]-dCTP (Witke et al., 1995). RNA was prepared by standard methods as well. Immunoblotting was performed after SDS-PAGE of protein extracts from various organs of the mice, using two different anti-CapG antibody preparations, a polyclonal antibody against gelsolin (Witke et al., 1995), and a polyclonal antibody against CapZ (gift of John Cooper, Washington University, St. Louis, MO).

Generation of double knockout mice lacking both CapG and gelsolin

Homozygous gelsolin knockout mice (Gsn$^{-/-}$) were bred with homozygous CapG knockout mice (CapG$^{-/-}$) to obtain double heterozygous mice, and then breedings and genotyping were performed to obtain Gsn$^{-/-}$ CapG$^{-/-}$ mice. In these mixed strains there was Mendelian segregation of alleles for both genes, and double-null mice were readily obtained.

Fibroblast culture and staining

Dermal fibroblasts were cultured as explants from the cutaneous tissue of 6-wk-old adult mice, and were maintained in DME with 10% fetal calf serum. To visualize the actin stress fibers, cells were cultured on glass coverslips coated with poly-L-lysine, fixed with acetone at −20°C for 5 min, and then incubated in 1 μg/ml of rhodamine-conjugated phalloidin for 20 min followed by three washes with PBS.

Inflammatory response by neutrophils

Sodium thioglycollate (1 ml at 2.4%) was injected into the peritoneal cavity of 6–8-wk-old mice, and the mice were killed at serial time points. The peritoneal cavity was then rinsed with 5 ml of PBS and the number of neutrophils was quantitated.

Isolation and culturing of mouse bone marrow macrophages

The lumen of fractured femurs from 6–8-wk-old female mice were flushed with 5–10 ml cell media (RPMI 1640 containing 10% fetal calf serum, 1% glutamate, 15 mM of Hepes, pH 7.5, and 100 U/ml and 100 mg/ml concentrations of penicillin and streptomycin, respectively). The effluent was cooled to 4°C and then centrifuged for 30 s at 100 *g* to remove tissue particles. The resulting supernatant was then centrifuged at 500 *g* for 15 min, and the resulting pellet was resuspended in 6 ml tissue culture medium. Aliquots (1 ml) containing ~10^6 cells were placed in 35-mm Petri dishes fitted with a 25-mm glass coverslip. The medium was then supplemented either with a final concentration of 1 ng/ml murine granulocyte MCSF (GMCSF; Sigma-Aldrich) or with 1/3 volume of supernatant from L. cells grown in the same media. Dishes were incubated at 37°C for 7 d, at which time the bone marrow monocytes had matured into macrophages.

Bone marrow macrophage motility studies

Ruffling analysis. Cells were grown on glass coverslips. 24 h before ruffling studies, cells were incubated in media without MCSF. To stimulate ruffling cells, a final concentration of 1 mg/ml of MCSF was added to the media and after 5 min cells were fixed with 3.7% formalin for 20 min at room temperature, permeabilized with 0.02% Triton X-100, and stained with 0.33 mM rhodamine-phalloidin. Cells were then analyzed under fluorescence microscopy using a Nikon Diaphote microscope. In some experiments, images were also captured in 0.3-mm optical section using a confocal microscope (Bio-Rad Laboratories). As described previously (Cox et al., 1997), ruffling was defined by the presence of F-actin–rich submembranous folds. The extent of ruffling of each cell was determined by a blinded observer (F.S. Southwick). Cells were scored on a scale of 0–2, where 0 indicates no ruffles were present, 1 indicates ruffling confined to one half of the cells′ dorsal surface, and 2 indicates ruffling of the entire dorsal surface. For each condition, 100 macrophages were analyzed. To examine stimulation of ruffling by *Salmonella*, American Type Culture Collection strain 1402c at a concentration of 10^7 organisms was incubated for 15 min with 10^6 macrophages adherent to a glass coverslip. Cells were then fixed with formalin and stained with rhodamine-phalloidin (as described above) and compared with similarly stained macrophages not exposed to *Salmonella*. Cells were also observed by phase–contrast microscopy to determine whether giant phagolysosomes containing *Salmonella* bacteria were present.

Phagocytosis. Fluorescently labeled zymosan was opsonized with IgG using the manufacturer's protocol (Bioparticle opsonizing reagent, rabbit antizymosan IgG; Molecular Probes). For complement-mediated phagocytosis, mouse serum was first incubated with zymosan particles (5×10^6 particles/ml) for 30 min at 4°C to bind IgG, and these beads were removed by centrifugation at 3,700 rpm. The resulting supernatant depleted of IgG was incubated with new zymosan beads for 1 h at 37°C to bind complement. Particles then were washed with 2× PBS . A ratio of 50 particles/cell was incubated with bone marrow macrophages adherent to glass for various times, cooled to 4°C, and external particles were quenched by adding 0.4% trypan blue as described previously (Hed, 1986). The number of fluorescent particles per cell was then determined for 100 cells, and the mean number of particles per cell was determined for each time point. The number of particles attached to, but not internalized by macrophages was determined as described previously (Serrander et al., 2000).

Vesicle rocketing. Coverslips containing adherent bone marrow macrophages were placed in buffer containing 135 mM NaCl and 15 mM Hepes, pH 7.25. Using 100 mM $LaCl_3$ stock solution, this buffer solution was brought to 1 mM $LaCl_3$, and after 10 min, the lanthanum-containing solution was removed by aspiration and replaced by an equal volume buffer containing 0.1 mM $LaCl_3$ and 1 mM $ZnCl_2$. After ~20 min, large motile vesicles were observed within the cytoplasm of the treated macrophages (Zeile et al., 2000).

Measurement of cytosolic-free Ca^{2+} in macrophages

Bone marrow macrophages were incubated for 30 min with a final concentration of 2 mM Fura-2, AM (Molecular Probes) in PBS containing 1 mM $CaCl_2$. Cells were then washed with calcium containing PBS and exposed to 20 ng/ml of PAF. Calcium was measured by ratio fluorescence imaging using an inverted microscope equipped with a cooled CCD camera (Arnaudeau et al., 2001), and $[Ca^{2+}]_i$ was calculated as described previously (Demaurex et al., 1992).

We would like to thank Dr. Daniel L. Purich for his helpful suggestions, and Dr. Nicolas Demaurex for performing the Fura-2 investigations.

This manuscript was funded by the National Institutes of Health (RO1AI/GM 23262, RO1HL54188) and a grant from the Zyma Research Foundation.

Submitted: 31 January 2001
Revised: 5 July 2001
Accepted: 6 July 2001

References

Alpuche-Aranda, C.M., E.L. Racoosin, J.A. Swanson, and S.I. Miller. 1994. *Salmonella* stimulate macrophage macropinocytosis and persist within spacious phagosomes. *J. Exp. Med.* 179:601–608.

Amatruda, J.F., J.F. Cannon, K. Tatchell, C. Hug, and J.A. Cooper. 1990. Disruption of the actin cytoskeleton in yeast capping protein mutants. *Nature.* 344: 352–354.

Arnaudeau, S., W.L. Kelley, J.V. Walsh, Jr., and N. Demaurex. 2001. Mitochondria recycle calcium to the endoplasmic reticulum and prevent the depletion of neighboring ER regions. *J. Biol. Chem.* 276:29430–29439.

Azuma, T., W. Witke, T.P. Stossel, J.H. Hartwig, and D.J. Kwiatkowski. 1998. Gelsolin is a downstream effector of rac for fibroblast motility. *EMBO J.* 17: 1362–1370.

Barkalow, K., W. Witke, D.J. Kwiatkowski, and J.H. Hartwig. 1996. Coordinated regulation of platelet actin filament barbed ends by gelsolin and capping protein. *J. Cell Biol.* 134:389–399.

Cooper, J.A., and D.A. Schafer. 2000. Control of actin assembly and disassembly at filament ends. *Curr. Opin. Cell Biol.* 12:97–103.

Cox, D., P. Chang, Q. Zhang, P.G. Reddy, G.M. Bokoch, and S. Greenberg.

1997. Requirements for both Rac1 and Cdc42 in membrane ruffling and phagocytosis in leukocytes. *J. Exp. Med.* 186: 1487–1494.

Crowley, M.R., K.L. Head, D.J. Kwiatkowski, H.L. Asch, and B.B. Asch. 2000. The mouse mammary gland requires the actin-binding protein gelsolin for proper ductal morphogenesis. *Dev. Biol.* 225:407–423.

Dabiri, G.A., C.L. Young, J. Rosenbloom, and F.S. Southwick. 1992. Molecular cloning of human macrophage capping protein cDNA. A unique member of the gelsolin/villin family expressed primarily in macrophages. *J. Biol. Chem.* 267:16545–16552.

Demaurex, N., W. Schlegel, P. Varnai, G. Mayr, D.P. Lew, and K.-H. Krause. 1992. Regulation of Ca^{2+} influx in myeloid cells. *J. Clin. Invest.* 90:830–839.

Garcia-del Portillo, F., and B.B. Finlay. 1994. *Salmonella* invasion of nonphagocytic cells induces formation of macropinosomes in the host cell. *Infect. Immun.* 62:4641–4645.

Hartwig, J.H., and T.P. Stossel. 1976. Interactions of actin, myosin, and an actin-binding protein of rabbit pulmonary macrophages. III. Effects of cytochalasin B. *J. Cell Biol.* 71:295–303.

Hed, J. 1986. Methods for distinguishing ingested from adhering particles. *Methods. Enzymol.* 132:198–204.

Heidemann, S.R., S. Kaech, R.E. Buxbaum, and A. Matus. 1999. Direct observations of the mechanical behaviors of the cytoskeleton in living fibroblasts. *J. Cell Biol.* 145:109–122.

Janmey, P.A., C. Chaponnier, S.E. Lind, K.S. Zaner, T.P. Stossel, and H.L. Yin. 1985. Interactions of gelsolin and gelsolin-actin complexes with actin. Effects of calcium on actin nucleation, filament severing, and end blocking. *Biochemistry.* 24:714–723.

Jones, B.D., H.F. Paterson, A. Hall, and S. Falkow. 1993. *Salmonella typhimurium* induces membrane ruffling by a growth factor-receptor-independent mechanism. *Proc. Natl. Acad. Sci. USA.* 90: 10390–10394.

Kwiatkowski, D.J. 1999. Functions of gelsolin: motility, signaling, apoptosis, cancer. *Curr. Opin. Cell Biol.* 11:103–108.

Li, E., T.H. Bestor, and R. Jaenisch. 1992. Targeted mutation of the DNA methyltransferase gene results in embryonic lethality. *Cell.* 69:915–926.

Lueck, A., D. Brown, and D.J. Kwiatkowski. 1998. The actin-binding proteins adseverin and gelsolin are both highly expressed but differentially localized in kidney and intestine. *J. Cell Sci.* 111:3633–3643.

Maekawa, S., and H. Sakai. 1990. Expression of scinderin, an actin filament-severing protein, in different tissues. *FEBS Lett.* 268:209–212.

Mazer, B.D., H. Sawami, A. Tordai, and E.W. Gelfand. 1992. Platelet-activated factor-mediated transmembrane signaling in human B lymphocytes is regulated through a pertussis- and cholera toxin-sensitive pathway. *J. Clin. Invest.* 90:759–765.

Prendergast, G.C., and E.B. Ziff. 1991. Mbh 1: a novel gelsolin/severin-related protein which binds actin in vitro and exhibits nuclear localization in vivo. *EMBO J.* 10:757–766.

Rudolph, M.G., C. Weise, S. Mirold, B. Hillenbrand, B. Bader, A. Wittinghofer, and W.D. Hardt. 1999. Biochemical analysis of SopE from *Salmonella typhimurium*, a highly efficient guanosine nucleotide exchange factor for RhoGTPases. *J. Biol. Chem.* 274:30501–30509.

Schafer, D.A., P.B. Jennings, and J.A. Cooper. 1996. Dynamics of capping protein and actin assembly in vitro: uncapping barbed ends by polyphosphoinositides. *J. Cell Biol.* 135:169–179.

Sechi, A.S., J. Wehland, and J.V. Small. 1997. The isolated comet tail pseudopodium of *Listeria* monocytogenes: a tail of two actin filament populations, long and axial and short and random. *J. Cell Biol.* 137:155–167.

Serrander, L., P. Skarman, B. Rasmussen, W. Witke, D.P. Lew, K.H. Krause, O. Stendahl, and O. Nusse. 2000. Selective inhibition of IgG-mediated phagocytosis in gelsolin-deficient murine neutrophils. *J. Immunol.* 165:2451–2457.

Southwick, F.S., and M.J. DiNubile. 1986. Rabbit alveolar macrophages contain a Ca^{2+}-sensitive, 41,000-dalton protein which reversibly blocks the "barbed" ends of actin filaments but does not sever them. *J. Biol. Chem.* 261:14191–14195.

Stossel, T.P. 1993. On the crawling of animal cells. *Science.* 260:1086–1094.

Sun, H.Q., K. Kwiatkowska, D.C. Wooten, and H.L. Yin. 1995. Effects of CapG overexpression on agonist-induced motility and second messenger generation. *J. Cell Biol.* 129:147–156.

Witke, W., A.H. Sharpe, J.H. Hartwig, T. Azuma, T.P. Stossel, and D.J. Kwiatkowski. 1995. Hemostatic, inflammatory, and fibroblast responses are blunted in mice lacking gelsolin. *Cell.* 81:41–51.

Young, C.L., A. Feierstein, and F.S. Southwick. 1994. Calcium regulation of actin filament capping and monomer binding by macrophage capping protein. *J. Biol. Chem.* 269:13997–14002.

Yu, F.X., P.A. Johnston, T.C. Sudhof, and H.L. Yin. 1990. gCap39, a calcium ion- and polyphosphoinositide-regulated actin capping protein. *Science.* 250: 1413–1415.

Zeile, W.L., D.L. Purich, and F.S. Southwick. 2000. Video microscopy: protocols for examining the actin-based motility of *Listeria*, *Shigella*, vaccinia, and lanthanum-induced endosomes. *In* Cytoskeleton: Signalling and Cell Regulation. K.L. Carraway and C.A.C Carraway, editors. Oxford University Press, Oxford. 140–142.

Zhou, D., M.S. Mooseker, and J.E. Galan. 1999. Role of the *S. typhimurium* actin-binding protein SipA in bacterial internalization. *Science.* 283:2092–2095.